

Bright light emissions with narrow spectral linewidths from single InAs/GaAs quantum dots directly grown on silicon substrates

M. Benyoucef, M. Usman, and J. P. Reithmaier

Citation: [Applied Physics Letters](#) **102**, 132101 (2013); doi: 10.1063/1.4799149

View online: <http://dx.doi.org/10.1063/1.4799149>

View Table of Contents: <http://scitation.aip.org/content/aip/journal/apl/102/13?ver=pdfcov>

Published by the [AIP Publishing](#)

Advertisement:



Goodfellow

metals • ceramics • polymers
composites • compounds • glasses

Save 5% • Buy online
70,000 products • Fast shipping

Bright light emissions with narrow spectral linewidths from single InAs/GaAs quantum dots directly grown on silicon substrates

M. Benyoucef,^{a)} M. Usman, and J. P. Reithmaier

Institute of Nanostructure Technologies and Analytics (INA), Center for Interdisciplinary Nanostructure Science and Technology (CINSA-T), University of Kassel, Heinrich-Plett-Str. 40, 34132 Kassel, Germany

(Received 15 November 2012; accepted 19 March 2013; published online 1 April 2013)

High brightness light emissions from single InAs/GaAs quantum dots (QDs) epitaxially grown directly on silicon substrates are realized for the first time. The grown structures contain a low quantum dot density of about 10^8 cm^{-2} . Low-temperature spatially resolved photoluminescence (PL) measurements illustrate bright single QD emissions with relatively sharp excitonic lines comparable to PL spectra of near-surface QDs grown on GaAs substrates. © 2013 American Institute of Physics. [<http://dx.doi.org/10.1063/1.4799149>]

Single quantum emitters have become an emerging area of fundamental research during the last years, driven by the need for non-classical light sources delivering single photons on demand for future implementation in the field of quantum information including quantum cryptography¹ and quantum computing.² The integration of classical optoelectronic devices on silicon is a long standing dream and keeps being a formidable challenge, as it is usually difficult to grow direct bandgap compound semiconductors on silicon. Silicon is the main material for various semiconductor devices; however, indirect nature of the silicon band structure prevents the realization of efficient light emitting devices. On the other hand, III–V materials, due to their excellent optical properties and optoelectronic capabilities, are widely utilized in conventional photonic devices such as lasers and LEDs. Integration of III–V semiconductor compound light sources with silicon^{3–11} is highly sought for the realization of photonic integrated circuits using the well-established complementary metal-oxide-semiconductor (CMOS) fabrication technologies. In particular, optical interconnect systems^{12,13} provide a promising approach for the realization of the next generation high-speed communication and computing technologies.

In the last decades, different approaches have been utilized such as SiGe/Si short period superlattices¹⁴ or defect atoms (e.g., rare earth atoms)¹⁵ to allow optical transitions in silicon matrix. Recently, several approaches are under exploration based on a hybrid combination of III–V and silicon material, e.g., by nanowire growth,¹⁶ wafer fusion techniques,¹⁷ using thick relaxation layers,¹⁸ or applying lattice matched material compositions.¹⁹ However, the growth of these buffer layers increases the process complexity and material cost.

For III–V/Si hybrid integration, direct epitaxial growth of III–V compounds on silicon substrates would be the most desirable approach, because only silicon processing is required as is already used in passive silicon photonics. Nevertheless, heteroepitaxial growth typically introduces a substantial crystalline defect density.^{20–22} As a result, the presence of high-density threading dislocations due to the lattice mismatch and the formation of antiphase boundaries

due to the polar–nonpolar nature of the III–V/IV semiconductor system propagating through the active material will become a non-radiative recombination centre.^{23–25} Because of such difficulties, most of the work concerning single quantum dots (QDs) and photon statistics has been done on III–V materials such as (In,Ga)As QDs embedded in GaAs matrix or integrated in microcavities,^{26–28} and few studies on II–VI compounds^{29–31} have been reported. These are rather expensive substrates; therefore, from the technological point of view, it would be desirable to obtain single-photons on demand from single quantum dots grown on conventional silicon substrate substrates. Recently, Benyoucef *et al.*³² have reported on the observation of triggered single-photon emission from a single CdTe QD embedded in a ZnTe layer grown on Si(001), but single or ensemble QD emission directly grown on silicon has not been reported so far.

In this letter, we report to our knowledge for the first time on the observation of bright photoluminescence (PL) emissions from single InAs/GaAs QDs grown directly on silicon substrates. After the substrate cleaning at 800°C for few minutes followed by deposition of a very thin GaAs/InAs/GaAs layer and using proper growth conditions described below, we have obtained well separated nanostructures with low dot density of about 10^8 cm^{-2} . The atomic force microscopy (AFM) investigations illustrate average III–V nanostructure heights of about 50–90 nm. Micro-photoluminescence (μ PL) measurements on individual QDs reveal their high optical properties with narrow linewidths.

The studied samples were grown by a GEN II Varian molecular beam Epitaxy (MBE) system on 5° miscut (100) silicon substrates. The silicon substrates were first *ex-situ* cleaned using standard buffered HF solution for 2 min as a pre-removal step of the surface native oxide and rinsed in de-ionized water prior the growth. This step produced a passivated hydrogen terminated silicon surface. In the *ex-situ* cleaning, all samples were then loaded in MBE entry/exit chamber within 10 min of *ex-situ* chemical cleaning. A 15 min de-gassing in buffer chamber was carried out before loading the samples in the growth chamber. The final thermal oxide desorption was done in the growth chamber.

After the surface preparation, the III–V nanostructures were directly grown on silicon. In this study, four different

^{a)} Author to whom correspondence should be addressed. Electronic mail: m.benyoucef@physik.uni-kassel.de

samples were grown named as A, B, C, and D for convenience, each of them representing subsequent growth steps for the formation of InAs/GaAs core-shell QDs formed on silicon. For each of these samples, an *in-situ* thermal annealing step of the silicon substrate was performed at 800 °C for few minutes to desorb the native oxides and to get rid of hydrogen passivation from silicon surface. For sample A, 4 monolayers (MLs) of GaAs were deposited at 600 °C. Using such high substrate temperature helps to achieve well-separated and low-density GaAs islands. For sample B, the same growth steps were performed as for sample A but continued by the deposition of a 3 MLs thick InAs layer at 500 °C. Due to the high strain between silicon and InAs, we expect that InAs is only grown on top of the GaAs islands formed in the previous growth step. For sample C, the GaAs/InAs QDs system was capped in addition with a 4 MLs thick GaAs layer at the same InAs growth temperature of 500 °C. Finally for sample D, the GaAs/InAs/GaAs structures were additionally capped with a nominal deposition of 2 MLs of GaAs at 600 °C. Then after few minutes, the sample was cooled down and taken out from the MBE chamber. All samples were studied by AFM to characterize the surface morphology. The final GaAs/InAs/GaAs QD structure (sample D) was used for optical investigations.

The μ PL measurements are performed at 5 K. The sample is mounted in a helium flow cryostat which can be moved by computer controlled xy-linear stages with spatial resolution of 100 nm. A microscope objective (NA = 0.7) is used to focus a continuous wave (cw) laser with an excitation wavelength of 532 nm. The same microscope objective was used to collect the QD emissions. The collected luminescence was then spectrally filtered by a 0.75 m focal length monochromator equipped with a liquid nitrogen cooled charge coupled device.

To investigate the morphology of the grown structures, we have performed AFM measurements. Figures 1(a)–1(d) show 2D and 3D AFM images ($5 \times 5 \mu\text{m}^2$) of the grown structures at four different growth stages. Well separated nanostructures with low dot density of about 10^8 cm^{-2} are observed for samples A, C, and D using optimized growth conditions. In the following, we will discuss with some detail the four growth phases.

Figure 1(a) displays low density GaAs islands obtained after the deposition of 4 MLs of GaAs at 600 °C. At such quite high substrate temperature, the ripening effect occurs, which results in the disappearance of small islands and formation of relatively large GaAs islands with average heights and lateral sizes of about 35 nm and 150 nm, respectively. It should be noted that a low silicon surface roughness value of about 0.2–0.3 nm was measured, which is comparable to the roughness for silicon substrates before growth. Then the growth temperature is decreased to 500 °C and 3 MLs of InAs were deposited. Due to the lower strain between InAs and GaAs compared to the silicon, InAs will preferably grow on GaAs islands. AFM images of Fig. 1(b) demonstrate increased island heights and sizes due to the growth of InAs on the low density GaAs; in addition, relatively high density small InAs islands are also grown on silicon substrates. In the next step, 4 MLs of GaAs were deposited at the same substrate temperature as for the InAs deposition to avoid a

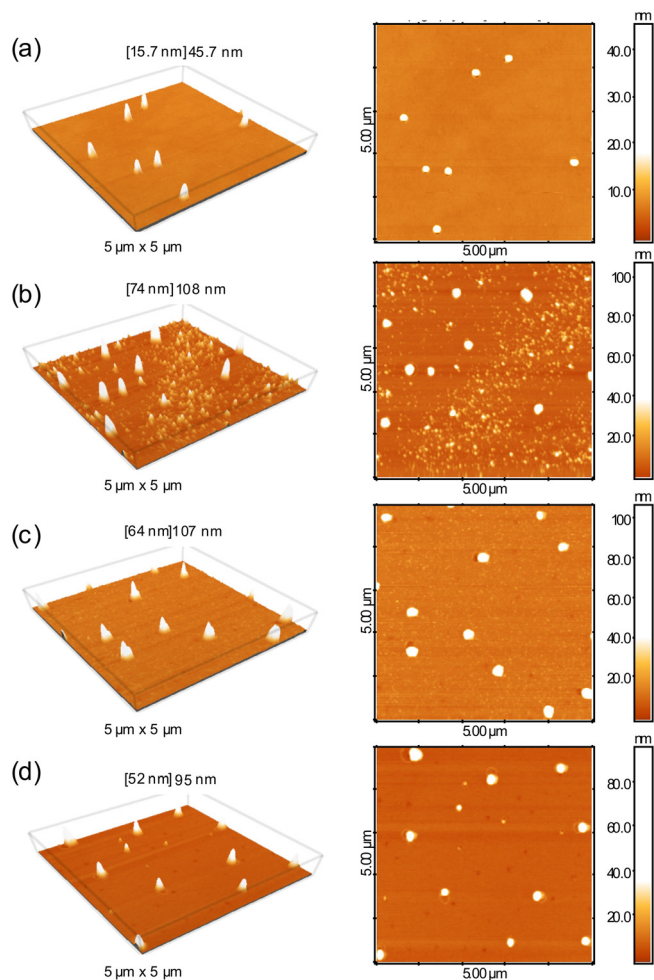


FIG. 1. 2D and 3D AFM images of the grown structures: (a) sample (A) with only 4 MLs of GaAs deposited at 600 °C, (b) sample (B) similar to (A) with additionally 3 MLs of InAs deposited at 500 °C, (c) sample (C) similar to (B) with an additional GaAs capping layer deposited at the same InAs growth temperature and (d) Sample (D) similar to (C) with additional 2 MLs of GaAs deposited at 600 °C for improved capping.

high indium desorption rate, which takes place above 500 °C on GaAs substrates (Fig. 1(c)). However, the desorption rate for small InAs islands directly formed on the silicon surface might be significantly higher which leads to considerable reduction of these islands and no additional dots are visible in (c) between the larger dots.

AFM images in Fig. 1(d) display the final growth step (Sample D). In this step, the structure in Fig. 1(c) was additionally capped with a nominal deposition of 2 MLs of GaAs at 600 °C. The average height of these islands is almost as twice large compared to the islands in the first growth step caused by the accumulations of III-V material. Due to such high substrate temperature, the previously formed InAs/GaAs nanostructures on silicon are completely desorbed and only large GaAs/InAs/GaAs structures are preserved with a similar density of sample A.

To examine the optical properties of the grown QD structures, we performed μ PL measurements on sample D using a grating with 600 lines/mm. The laser spot size is around $1 \mu\text{m}^2$ and due to the low QD density, it was possible to detect PL emissions from single QDs without a need to process mesa structures.

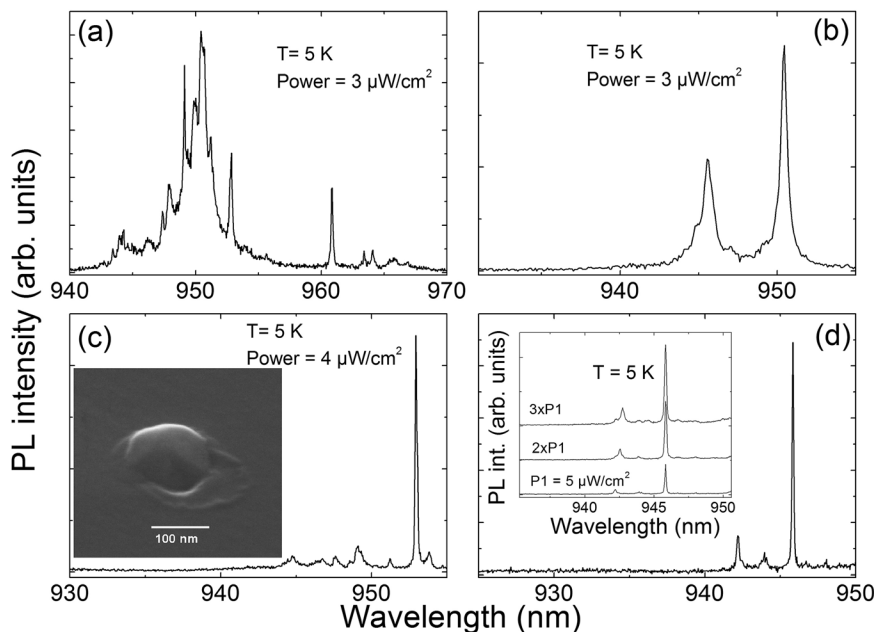


FIG. 2. PL spectra of InAs/GaAs QDs (a–d) were taken from four different locations of the sample at low laser excitation powers. The inset of (c) shows a scanning electron microscope image of a single InAs/GaAs QD grown directly on silicon. The inset of (d) illustrates the PL spectra taken at three different excitation laser powers.

Figures 2(b)–2(d) show PL emission from three different QDs taken at low excitation powers. The PL spectrum in Fig. 2(a) taken at an excitation power of about $3 \mu\text{W}/\text{cm}^2$ is most likely originated from the emissions of few coalesced QDs which result in a broad PL linewidth with few sharp peaks. Figure 2(b) displays a PL spectrum of a QD with two well separated peaks. The energy difference between the two peaks is in the order of 6–7 meV which is slightly larger compared to the biexciton binding energy of GaAs-based QDs. The PL linewidth of the intense line is about $500 \mu\text{eV}$. This linewidth broadening could be due to the less GaAs material capping or to nonradiative recombination channels caused by defects that could propagate from silicon substrates. Further investigations are necessary to get better understanding of the mechanisms responsible for the line broadening. Figures 2(c) and 2(d) show typical PL spectra from single InAs/GaAs QDs grown directly on silicon substrates. Both spectra were taken at low excitation powers and display very sharp PL lines with almost no background. The inset of Fig. 2(c) shows a scanning electron microscope image of a faceted single InAs/GaAs QD grown directly on silicon.

The measured PL linewidths are ranging from 150 to $200 \mu\text{eV}$ which are comparable to PL linewidths of our grown near-surface single InAs QDs on GaAs substrate. The relatively broad excitonic linewidths could be due to coupling of QD and surface states. The inset of Fig. 2(d) shows the PL spectra taken at three different excitation laser powers of the same QD in Fig. 2(d). Increasing the laser power from $5 \mu\text{W}/\text{cm}^2$ to $15 \mu\text{W}/\text{cm}^2$ results in a slight linewidth broadening of about $50 \mu\text{eV}$ and no peak energy shift is detectable for this specific QD. The PL intensities of the two lines show an exciton-biexciton behavior. It should be also noted that the biexciton binding energy is around 5 meV which is comparable to the biexciton binding energy in GaAs-based QDs. This is an indication that the GaAs materials have formed a shell around the InAs leading to the formation of InAs/GaAs QDs. This was also confirmed by the AFM measurements in Fig. 1(d) as discussed above. However, if one assumes that the InAs was not capped with GaAs in Fig. 1(c) then by growing additional GaAs at 600°C (Fig. 1(d))

will lead to completely desorbing the InAs material which is not the case as proven by the μPL measurements. This is a strong indication that the InAs is surrounded by GaAs. Based on these results, the PL emissions (Figs. 2(c) and 2(d)) with narrow linewidths are most probably originated from defect free single QDs. Further transmission electron microscopy (TEM) investigations are necessary to get more information and a deeper understanding for the grown QD structures.

In conclusion, we have demonstrated bright single InAs/GaAs QD emissions with narrow PL linewidths grown directly on silicon substrates. We have also shown the grown structures contain a low QD density of about 10^8cm^{-2} . These results indicate that it may become feasible to fabricate single-photon sources for quantum information processing on low cost basis. Further position controlled high-resolution AFM and polarization dependent μPL studies are necessary to understand also the correlation between the morphology, like faceting and shape, with the spectral properties of individual dots.

By enlarging the InAs core part of the QDs, also longer emission wavelengths should be feasible, which may cover in future also the telecom wavelength range. Further work is now focusing on increasing the dot density and to embed them fully in a silicon matrix. First morphology studies by TEM are very promising but will be reported elsewhere. The development of such a new III-V-Si-hybrid material could be a very promising new path towards the realization of a fully CMOS compatible fabrication process of integrated optoelectronics on silicon.

We acknowledge A. Dirk, K. Fuchs, F. Schnabel, A. Gushterov, and M. Yacob for technical support. This work was supported by the BMBF (projects Monalisa and QuaHL-Rep).

¹C. H. Brassard and G. Bennet, in *Proceedings of IEEE International Conference on Computers, Systems and Signal Processing, Bangalore, India* (1984), pp. 175–179.

²D. Loss and D. P. DiVincenzo, *Phys. Rev. A* **57**, 120 (1998).

³R. Heitz, N. Ledentsov, D. Bimberg, A. Egerov, M. Maximov, V. Ustinov, A. Zhukov, Z. Alverov, G. Cirilin, I. Soshikov, N. Zakharov, P. Werner, and U. Gösele, *Appl. Phys. Lett.* **74**, 1701 (1999).

- ⁴C. Seassal, P. Rojo-Romeo, X. Letartre, P. Viktorovitch, G. Hollinger, E. Jalaguier, S. Pocas, and B. Aspar, *Electron. Lett.* **37**, 222 (2001).
- ⁵C. Monat, C. Seassal, X. Letartre, P. Viktorovitch, P. Regreny, M. Gendry, P. Rojo-Romeo, G. Hollinger, E. Jalaguier, S. Pocas, and B. Aspar, *Appl. Phys. Lett.* **81**, 5102 (2002).
- ⁶S. Palit, J. Kirch, G. Tsviid, L. Mawst, T. Kuech, and N. Jokerst, *Opt. Lett.* **34**, 2802 (2009).
- ⁷K. Tanabe, D. Guimard, D. Bordel, S. Iwamoto, and Y. Arakawa, *Opt. Express* **18**, 10604 (2010).
- ⁸J. Yoon, S. Jo, I. S. Chun, I. Jung, H.-S. Kim, M. Meitl, E. Menard, X. Li, J. J. Coleman, U. Paik, and J. A. Rogers, *Nature* **465**, 329 (2010).
- ⁹R.-H. Kim, D.-H. Kim, J. Xiao, B. H. Kim, S.-I. Park, B. Panilaitis, R. Ghaffari, J. Yao, M. Li, Z. Liu, V. Malyarchuk, D. G. Kim, A.-P. Le, R. G. Nuzzo, D. L. Kaplan, F. G. Omenetto, Y. Huang, Z. Kang, and J. A. Rogers, *Nature Mater.* **9**, 929 (2010).
- ¹⁰H. Ko, K. Takei, R. Kapadia, S. Chuang, H. Fang, P. W. Leu, K. Ganapathi, E. Plis, H. S. Kim, S. Y. Chen, M. Madsen, A. C. Ford, Y. L. Chueh, S. Krishna, S. Salahuddin, and A. Javey, *Nature* **468**, 286 (2010).
- ¹¹R. Chen, T.-T. D. Tran, K. W. Ng, W. S. Ko, L. C. Chuang, F. G. Sedgwick, and C. Chang-Hasnain, *Nature Photon.* **5**, 170 (2011).
- ¹²D. A. B. Miller, *Proc. IEEE* **88**, 728 (2000).
- ¹³J. W. Goodman, F. J. Leonberger, S. Y. Kung, and R. A. Athale, *Proc. IEEE* **72**, 850 (1984).
- ¹⁴G. Abstreiter, *Phys. Scr.* **T49A**, 42 (1993).
- ¹⁵M. Castagna, S. Coffa, M. Monaco, L. Caristia, A. Messina, R. Mangano, and C. Bongiorno, *Physica E* **16**, 547 (2003).
- ¹⁶T. Mårtensson, C. Svensson, B. Wacaser, M. Larsson, W. Seifert, K. Deppert, A. Gustafsson, L. Wallenberg, and L. Samuelson, *Nano Lett.* **4**, 1987 (2004).
- ¹⁷M. Heck, H. Chen, A. Fang, B. Koch, D. Liang, H. Park, M. Sysak, and J. Bowers, *IEEE J. Sel. Top. Quantum Electron.* **17**, 333 (2011).
- ¹⁸Z. Mi, J. Yang, P. Bhattacharya, G. Qin, and Z. Ma, *Proc. IEEE* **97**, 1239 (2009).
- ¹⁹S. Liebich, M. Zimprich, A. Beyer, C. Lange, D. Franzbach, S. Chatterjee, N. Hossain, S. Sweeney, K. Volz, B. Kunert, and W. Stolz, *Appl. Phys. Lett.* **99**, 071109 (2011).
- ²⁰H. Kroemer, T. Liu, and P. Petroff, *J. Cryst. Growth* **95**, 96 (1989).
- ²¹M. Sugo, Y. Takanashi, M. M. Aljassim, and M. Yamaguchi, *J. Appl. Phys.* **68**, 540 (1990).
- ²²Y. Shimizu and Y. Okada, *J. Cryst. Growth* **265**, 99 (2004).
- ²³L. Li, D. Guimard, M. Rajesh, and Y. Arakawa, *Appl. Phys. Lett.* **92**, 263105 (2008).
- ²⁴Z. M. Zhao, O. Hulko, T. Yoon, and Y. Xie, *J. Appl. Phys.* **98**, 123526 (2005).
- ²⁵Y. Wang, J. Zou, Z. Zhao, Z. Hao, and K. Wang, *Nanotechnology* **20**, 305301 (2009).
- ²⁶J. M. Gérard and B. Gayral, *J. Lightwave Technol.* **17**, 2089 (1999).
- ²⁷M. Benyoucef, S. M. Ulrich, P. Michler, J. Wiersig, F. Jahnke, and A. Forchel, *J. Appl. Phys.* **97**, 023101 (2005).
- ²⁸E. Moreau, I. Robert, J. M. Gérard, I. Abram, L. Manin, and V. Thierry-Mieg, *Appl. Phys. Lett.* **79**, 2865 (2001).
- ²⁹S. M. Ulrich, S. Strauf, and P. Michler, G. Bacher, and A. Forchel, *Appl. Phys. Lett.* **83**, 1848 (2003).
- ³⁰T. Aichele, V. Zwiller, O. Benson, I. Akimov, and F. Henneberger, *J. Opt. Soc. Am. B* **20**, 2189 (2003).
- ³¹C. Couteau, S. Moehl, F. Tinjod, J. M. Gérard, K. Kheng, and H. Mariette, *Appl. Phys. Lett.* **85**, 6251 (2004).
- ³²M. Benyoucef, H. S. Lee, J. Gabel, H. L. Park, T. W. Kim, A. Rastelli, and O. G. Schmidt, *Nano Lett.* **9**, 304 (2009).